ON THE FEASIBILITY OF CROSS-TASK TRANSFER WITH MODEL-BASED REINFORCEMENT LEARNING

Anonymous authors
Paper under double-blind review

ABSTRACT

Reinforcement Learning (RL) algorithms can solve challenging control problems directly from image observations, but they often require millions of environment interactions to do so. Recently, model-based RL algorithms have greatly improved sample-efficiency by concurrently learning an internal model of the world, and supplementing real environment interactions with imagined rollouts for policy improvement. However, learning an effective model of the world from scratch is challenging, and in stark contrast to humans that rely heavily on world understanding and visual cues for learning new skills. In this work, we investigate whether internal models learned by modern model-based RL algorithms can be leveraged to solve new, distinctly different tasks faster. We propose Model-Based **Cross**-Task **Tra**nsfer (**XTRA**), a framework for sample-efficient online RL with scalable pretraining and finetuning of learned world models. By proper pretraining and concurrent cross-task online fine-tuning, we achieve substantial improvements over a baseline trained from scratch; we improve mean performance of model-based algorithm EfficientZero by 23%, and by as much as 71% in some instances.

1 INTRODUCTION

Reinforcement Learning (RL) has achieved great feats across a wide range of areas, most notably game-playing (Mnih et al., 2013; Silver et al., 2016; Berner et al., 2019; Cobbe et al., 2020). However, traditional RL algorithms often suffer from poor sample-efficiency and require millions (or even billions) of environment interactions to solve tasks – especially when learning from high-dimensional observations such as images. This is in stark contrast to humans that have a remarkable ability to quickly learn new skills despite very limited exposure (Dubey et al., 2018). In an effort to reliably benchmark and improve the sample-efficiency of image-based RL across a variety of problems, the Arcade Learning Environment (ALE; (Bellemare et al., 2013)) has become a long-standing challenge for RL. This task suite has given rise to numerous successful and increasingly sample-efficient algorithms (Mnih et al., 2013; Badia et al., 2020; Kaiser et al., 2020; Schrittwieser et al., 2020; Kostrikov et al., 2021; Hafner et al., 2021; Ye et al., 2021), notably most of which are model-based, *i.e.*, they learn a *model* of the environment (Ha & Schmidhuber, 2018).

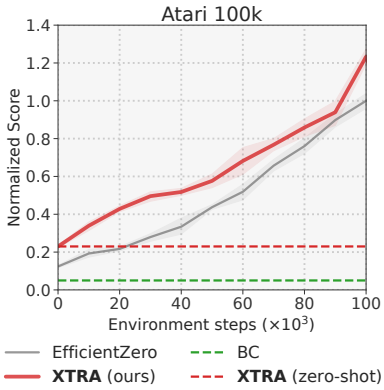

Figure 1. **Aggregated Atari 100k scores** normalized by mean EfficientZero score at 100k environment steps across 10 games and 5 seeds.

Most recently, EfficientZero Ye et al. (2021) – a model-based RL algorithm – has demonstrated impressive sample-efficiency, surpassing human-level performance with as little as 2 hours of real-time game play in select Atari 2600 games from the ALE. This achievement is attributed – in part – to the algorithm concurrently learning an internal *model* of the environment from interaction, and using the learned model to *imagine* (simulate) further interactions for planning and policy improvement, thus reducing reliance on real environment interactions for skill acquisition. However, current RL algorithms – including EfficientZero – are still predominantly assumed to learn both perception, model, and skills *tabula rasa* (from scratch) for each new task. On the contrary, humans rely heavily on prior knowledge and visual cues when learning new skills. For example, a study found that human players easily pick up on visual cues about game mechanics and objectives when exposed to a

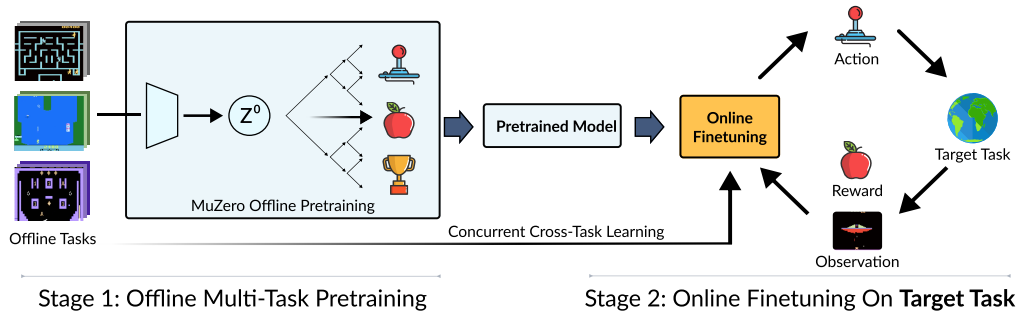

Figure 2. Model-Based **Cross**-Task **Tra**nsfer (**XTRA**): a sample-efficient online RL framework with scalable pretraining and finetuning of learned world models using auxiliary data from offline tasks.

video game for the very first time, and that human performance is severely degraded if such cues are removed or conflict with prior experiences (Dubey et al., 2018).

In related areas such as computer vision and natural language processing, large-scale unsupervised/self-supervised/supervised pretraining on large-scale datasets (Devlin et al., 2019; Brown et al., 2020; Li et al., 2022; Radford et al., 2021; Chowdhery et al., 2022) has emerged as a powerful framework for solving numerous downstream tasks with few samples (Alayrac et al., 2022). This pretraining paradigm has recently been extended to visuo-motor control in various forms, *e.g.*, by leveraging *frozen* (no finetuning) pretrained representations (Xiao et al., 2022; Parisi et al., 2022) or by finetuning in a supervised setting (Reed et al., 2022; Lee et al., 2022). However, the success of finetuning for *online RL* has mostly been limited to same-task initialization of model-free policies from offline datasets (Wang et al., 2022; Zheng et al., 2022), or adapting policies to novel instances of a given task (Mishra et al., 2017; Julian et al., 2020; Hansen et al., 2021a), with prior work citing high-variance objectives and catastrophical forgetting as the main obstacles to finetuning representations with RL (Bodnar et al., 2020; Xiao et al., 2022).

In this work, we explore whether such positive transfer can be induced with current model-based RL algorithms in an *online* RL setting, and across *markedly distinct* tasks. Specifically, we seek to answer the following questions: *when* and *how* can a model-based RL algorithm such as EfficientZero benefit from pretraining on a diverse set of tasks? We base our experiments on the ALE due to cues that are easily identifiable to humans despite great diversity in tasks, and identify two key ingredients – cross-task finetuning and task alignment – for model-based adaptation that improve sample-efficiency substantially compared to models learned tabula rasa. In comparison, we find that a naïve treatment of the finetuning procedure as commonly used in supervised learning (Pan & Yang, 2010; Doersch et al., 2015; He et al., 2020; Reed et al., 2022; Lee et al., 2022) is found to be unsuccessful or outright *harmful* in an RL context.

Based on our findings, we propose Model-Based **Cross**-Task **Tra**nsfer (**XTRA**), a framework for sample-efficient online RL with scalable pretraining and finetuning of learned world models using extra, auxiliary data from other tasks (see Figure 2). Concretely, our framework consists of two stages: *(i) offline multi-task pretraining* of a world model on an offline dataset from m diverse tasks, a *(ii) finetuning* stage where the world model is jointly finetuned on a *target task* in addition to m offline tasks. By leveraging offline data both in pretraining and finetuning, XTRA overcomes the challenges of catastrophical forgetting. To prevent harmful interference from certain offline tasks, we adaptively re-weight gradient contributions in unsupervised manner based on similarity to target task.

We evaluate our method and a set of strong baselines extensively across 14 Atari 2600 games from the Atari100k benchmark (Kaiser et al., 2020) that require algorithms to be extremely sample-efficient. From Figure 1 and Table 1, We observe XTRA improves sample-efficiency substantially across most tasks, improving mean and median performance of EfficientZero by 23% and 25%, respectively.

2 Background

Problem setting. We model image-based agent-environment interaction as an episodic Partially Observable Markov Decision Process (POMDP; Kaelbling et al. (1998)) defined by the tuple $\mathcal{M} = \langle \mathcal{O}, \mathcal{A}, \mathcal{P}, \rho, r, \gamma \rangle$, where $\mathcal{O}$ is the observation space (pixels), $\mathcal{A}$ is the action space, $\mathcal{P}\colon \mathcal{O} \times \mathcal{A} \mapsto \mathcal{O}$ is

a transition function, ρ is the initial state distribution, $r\colon \mathcal{O} \times \mathcal{A} \mapsto \mathbb{R}$ is a scalar reward function, and $\gamma \in [0, 1)$ is a discount factor. As is standard practice in ALE (Bellemare et al., 2013), we convert $\mathcal{M}$ to a fully observable Markov Decision Process (MDP; Bellman (1957)) by approximating state $\mathbf{s}_t \in \mathcal{S}$ at time t as a stack of frames $\mathbf{s}_t \doteq \{o_t, o_{t-1}, o_{t-2}, \dots\}$ where $o \in \mathcal{O}$ (Mnih et al., 2013), and redefine $\mathcal{P}, \rho, r$ to be functions of $\mathbf{s}$. Our goal is then to find a (neural) policy $\pi_\theta(\mathbf{a}|\mathbf{s})$ parameterized by θ that maximizes discounted return $\mathbb{E}_{\pi_\theta}[\sum_{t=1}^{t} \gamma_t r(\mathbf{s}_t, \mathbf{a}_t)]$ where $\mathbf{a}_t \sim \pi_\theta(\mathbf{a}|\mathbf{s}),\ \mathbf{s}_t \sim \mathcal{P}(\mathbf{s}_t, \mathbf{a}_t), \mathbf{s}_0 \sim \rho$, and T is the episode horizon. For clarity, we denote all parameterization by θ throughout this work. To obtain a good policy from minimal environment interaction, we learn a *"world model"* from interaction data and use the learned model for action search. Define $\mathcal{M}$ as the *target task* that we aim to solve. Then, we seek to first obtain a good parameter initialization θ that allows us to solve task $\mathcal{M}$ using fewer interactions (samples) than training from scratch, *i.e.*, we wish to improve the *sample-efficiency* of online RL. We do so by first pretraining the model on an *offline* (fixed) dataset that consists of transitions $(\mathbf{s}, \mathbf{a}, r, \mathbf{s}')$ collected by unknown behavior policies in m environments $\{\tilde{\mathcal{M}}^i \,|\tilde{\mathcal{M}}^i \neq \mathcal{M}, 1 \leq i \leq m\}$, and then *finetune* the model by online interaction on the target task.

EfficientZero (Ye et al., 2021) is a model-based RL algorithm based on MuZero (Schrittwieser et al., 2020) that learns a discrete-action latent dynamics model from environment interactions, and selects actions by lookahead via Monte Carlo Tree Search (MCTS; (Abramson, 1987; Coulom, 2006; Silver et al., 2016)) in the latent space of the model. Figure 3 provides an overview of the three main components of the MuZero algorithm: a representation (encoder) h_θ, a dynamics (transition) function g_θ, and a prediction head f_θ. Given an observed state $\mathbf{s}_t$, EfficientZero projects the state to a latent representation $\mathbf{z}_t = h_\theta(\mathbf{s}_t)$, and predicts future latent states $\mathbf{z}_{t+1}$ and instantaneous rewards $\hat{r}_t$ using an action-conditional latent dynamics function $\mathbf{z}_{t+1}, \hat{r}_t = g_\theta(\mathbf{z}_t, \mathbf{a}_t)$. For each latent state, a prediction network f_θ estimates a probability distribution $\hat{p}$ over (valid) actions $\mathbf{a} \in \mathcal{A}$, as well as the expected state value $\hat{v}$ of the given state, *i.e.*, $\hat{v}_t, \hat{p}_t = f_\theta(\mathbf{z}_t)$. Intuitively, h_θ and g_θ allow EfficientZero to search for actions entirely in its latent space before executing actions in the real environment, and f_θ predicts quantities that help guide the search towards high-return action sequences. Concretely, $\hat{v}$ provides a return estimate for nodes at the lookahead horizon (as opposed to truncating the cumulative sum of expected rewards) and $\hat{p}$ provides an action distribution prior that helps guide the search. We describe EfficientZero's learning objective between model prediction $(\hat{p}, \hat{v}, \hat{r})$ and quantity targets (π, z, u) in Appendix A EfficientZero improves the sample-efficiency of MuZero by introducing additional auxiliary losses during training. We adopt EfficientZero as our backbone model and learning algorithm, but emphasize that our framework is applicable to most model-based algorithms, including continuous action spaces (Hafner et al., 2019a; Hansen et al., 2022).

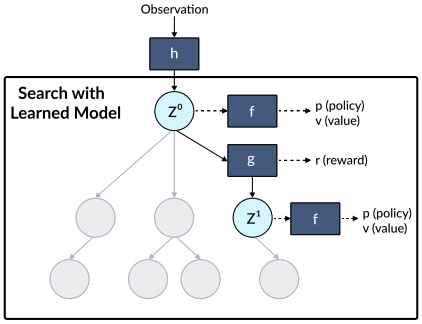

Figure 3. **MuZero/EfficientZero** combines MCTS with a learned representation network (h), latent dynamics function (g), and prediction head (f).

3 Model-Based Cross-Task Transfer

We propose Model-Based **Cross**-Task **Tra**nsfer (**XTRA**), a two-stage framework for offline multi-task pretraining and cross-task transfer of learned world models by finetuning with online RL. Specifically, we first pretrain a world model on offline data from a set of diverse pretraining tasks, and then iteratively finetune the pretrained model on data from a *target* task collected by online interaction. In the following, we introduce each of the two stages – pretraining and finetuning – in detail.

3.1 Offline Multi-Task Pretraining

In this stage, we aim to learn a single world model with general perceptive and dynamics priors across a diverse set of offline tasks. We emphasize, however, that the goal of pretraining is not to obtain a truly generalist agent, but rather to learn a good initialization for finetuning to unseen tasks. Learning a single RL agent for a diverse set of tasks is however difficult in practice, which is only exacerbated by extrapolation errors due to the offline RL setting (Kumar et al., 2020). To address the challenge of multi-task learning, we propose to pretrain the model following a *student-teacher* training setup

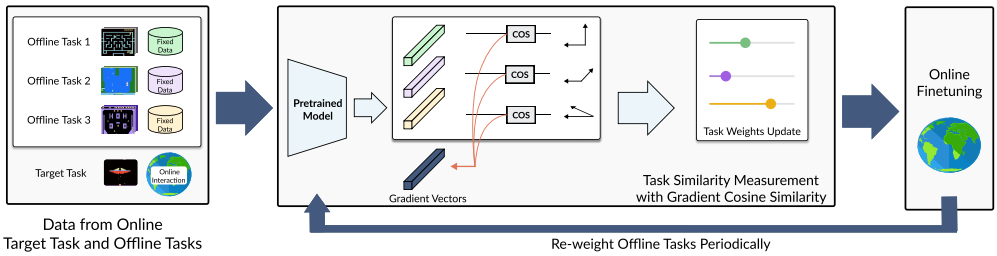

Figure 4. Illustration of our proposed **Concurrent Cross-Task Learning** strategy, where we selectively include a subset of the available pretraining tasks while finetuning on a target task.

in the same spirit to DQN multi-task policy distillation in Rusu et al. (2016) and Actor-Mimic in Parisotto et al. (2016) , where *teacher* models are trained separately by offline RL for each task, and then distilled into a single multi-task model using a novel instantiation of the MuZero Reanalyze (Schrittwieser et al., 2021) algorithm.

For each pretraining task we assume access to a fixed dataset $\{\tilde{\mathcal{D}}^i \,|1 \leq i \leq m\}$ that consists of trajectories from an unknown (and potentially sub-optimal) behavior policy. Importantly, we do *not* make any assumptions about the quality or the source of trajectories in the dataset, *i.e.*, we do not assume datasets to consist of expert trajectories. We first train individual EfficientZero *teacher* models on each dataset for a fixed number of iterations in a single-task (offline) RL setting, resulting in m *teacher* models $\{\tilde{\pi}^i_\psi \,|1 \leq i \leq m\}$. After training, we store the model predictions, $(\hat{p}, \hat{v})$, from each *teacher* model $\tilde{\pi}^i_\psi$ together with the environment reward u as student's quantity targets (π, z, u) respectively for a given game $\tilde{\mathcal{M}}^i$ (see Appendix A for the definition of each quantity). Next, we learn a *multi-task student* model π_θ by distilling the task-specific teachers into a single model via these quantity targets. Specifically, we optimize the student policy by sampling data uniformly from all pretraining tasks, and use value/policy targets generated by their respective teacher models rather than bootstrapping from student predictions as commonly done in the (single-task) MuZero Reanalyze algorithm. This step can be seen as learning multiple tasks simultaneously with direct supervision by distilling predictions from multiple teachers into a single model. Empirically, we find this to be a key component in scaling up the number of pretraining tasks. Although teacher models may not be optimal depending on the provided offline datasets, we find that they provide stable (due to fixed parameters during distillation) targets of sufficiently good quality. The simpler alternative – training a multi-task model on all m pretraining tasks simultaneously using RL is found to not scale beyond a couple of tasks in practice, as we will demonstrate our experiments in Appendix C. After distilling a multi-task student model, we now have a single set of pretrained parameters that can be used for finetuning to a variety of tasks via online interaction, which we introduce in the following section.

3.2 Online Finetuning on a Target Task

In this stage, we iteratively interact with a target task (environment) to collect interaction data, and finetune the pretrained model on data from the target task. However, we empirically observe that directly finetuning the pretrained model often leads to poor performance on the target task due to *catastrophical forgetting*. Specifically, the initial sub-optimal data collected from online target task will cause a large perturbation in the original pretrained model parameters, which often erases useful inductive priors learned during pretraining. To overcome this challenge, we propose concurrent cross-task learning strategy: we retain offline data from the pretraining stage, and concurrently finetune the model on both data from the target task, as well as data from the pretraining tasks. While this procedure addresses catastrophical forgetting, interference between the target task and certain pretraining tasks can be harmful for the sample-efficiency in online RL. As a solution, gradient contributions from offline tasks are periodically re-weighted in an unsupervised manner based on their similarity to the target task. Figure 4 shows the specific concurrent cross-task learning procedure for target task finetuning in our framework.

At each training step t, we jointly optimize the target online task $\mathcal{M}$ and m offline (auxiliary) tasks $\{\tilde{\mathcal{M}}^i \,|\tilde{\mathcal{M}}^i \neq \mathcal{M}, 1 \leq i \leq m\}$ that were used during the *offline multi-task pretraining* stage. Our online finetuning objective is defined as:

$$\mathcal{L}_t^{\text{adapt}}(\theta) = \mathcal{L}_t^{\text{ez}}(\mathcal{M}) + \sum_{i=1}^{m} \eta^i \mathcal{L}_t^{\text{ez}}(\tilde{\mathcal{M}}^i) \tag{1}$$

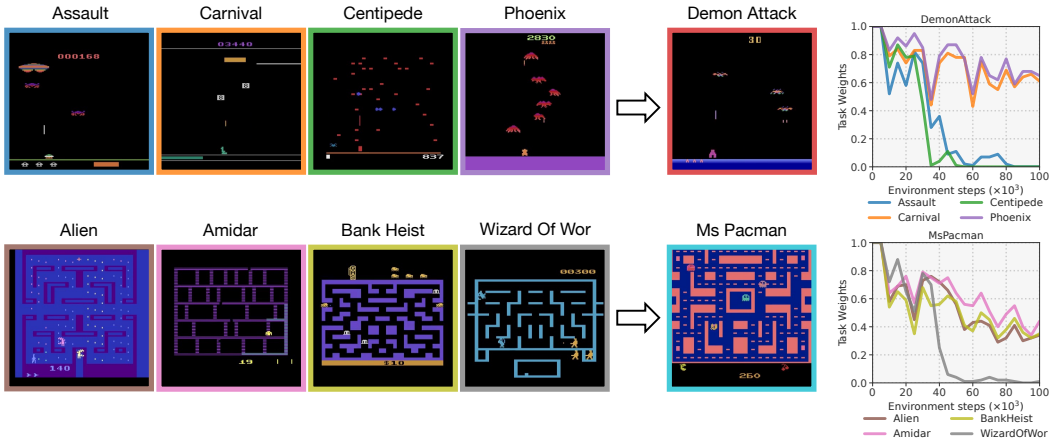

(a) Cross-Task Transfer from 4 offline games (left) to 1 target game (right). *(b)* Task weights.

Figure 5. **Visualization of Concurrent Cross-Task Learning.** (*left*) the model adapts to the online target game while concurrently learns 4 offline games. (*right*) the figure shows the task weights of the 4 offline games that are periodically recomputed based on their gradient similarity to the target games (DemonAttack and MsPacman).

where $\mathcal{L}^{\text{ez}}$ is the ordinary (single-task) EfficientZero objective (see Appendix A), and η^i are dynamically (and independently) updated task weights for each of the m pretraining tasks. The target task loss term maintains a constant task weight of 1. During online finetuning, we use distillation targets from teachers for offline pretrained games and MuZero Reanalysis to compute targets for online target task where we have no teacher.

In order to dynamically re-weight task weights η^i throughout the training process, we break down the total number of environment steps (*i.e.*, 100k in our experiments) into even T-step cycles (intervals). Within each cycle, we spend first N-steps to compute an updated η^i corresponding to each offline task $\tilde{\mathcal{M}}^i$. The new η^i will then be fixed during the remaining $T - N$ steps in the current cycle and the first N steps in the next cycle. We dynamically assign the task weights by measuring the "relevance" between each offline task $\tilde{\mathcal{M}}^i$ and the (online) target task $\mathcal{M}$. Inspired by the conflicting gradients measurement for multi-task learning in (Yu et al., 2020), we compute the cosine similarity between loss gradients $\tilde{\mathcal{G}}_n^i$ from $\mathcal{L}_n^{\text{ez}}(\tilde{\mathcal{M}}^i)$ and $\mathcal{G}_n$ from $\mathcal{L}_n^{\text{ez}}(\mathcal{M})$ given by

$$\text{Sim}(\tilde{\mathcal{M}}^i, \mathcal{M}) = \frac{\tilde{\mathcal{G}}_n^i \cdot \mathcal{G}_n}{\|\tilde{\mathcal{G}}_n^i\| \|\mathcal{G}_n\|} \,. \tag{2}$$

Within the N-step update, we maintain a task-specific counter s^i and the new task weights η^i can be reset by $\eta^i = \frac{s^i}{N}$ at the beginning of each every T-cycle. Procedure to obtain s^i is stated in Appendix B. Concretely, $\text{Sim}(\tilde{\mathcal{M}}^i, \mathcal{M})$ measures the angle between two task gradients $\tilde{\mathcal{G}}_n^i$ and $\mathcal{G}_n$. Intuitively, we aim to (approximately) prevent gradient contributions from the offline tasks from conflicting with the gradient update direction for the target task by regulating offline tasks objectives with task weights η. While re-weighting task weights at every gradient update would result in the least amount of conflicting gradients, it is prohibitively costly to do so in practice. However, we empirically find the cosine similarity of task gradients to be strongly correlated in time, *i.e.*, the cosine similarity does not change much between consecutive gradient steps. By instead updating task weights every N steps, our proposed technique mitigates gradient conflicts at a negligible computational cost in contrast to the compute-intensive gradient modification method proposed in (Yu et al., 2020). Figure 5 demonstrates adjustments of task weights during finetuning with visualizations from different pretraining and finetuning tasks.

4 Experiments

We evaluate our method and baselines on **14** tasks from the limited-interaction Atari100k benchmark (Kaiser et al., 2020) where only 100k environment steps are permitted. We seek to answer:

- When can we empirically expect finetuning to be successful?

Table 1. **Scores on the Atari 100k benchmark (*similar* pretraining tasks).** Methods are evaluated after 100k environment steps. For each game, XTRA is first pretrained on all other 4 games from the same category. Our main result is highlighted. We include three main ablation results by removing cross-task optimization in finetuning (only online RL), the pretraining stage (random initialization), or task weights assignment (constant weights). We also include zero-shot performance of our method for target tasks in comparison to a behavioral cloning baseline. All numbers are means of 5 seeds with 32 evaluation episodes.

Category	Game	BC (finetune)	Efficient Zero	Efficient Zero-L	XTRA (Ours)	Ablations (XTRA) w.o. cross-task	w.o. pretraining	w.o. task weights	Zero-Shot BC	Zero-Shot XTRA (Ours)
Shooter	Assault	838.4	1027.1	1041.6	**1294.6**	1246.4	1257.5	1164.2	0.0	92.8
	Carnival	1952.4	3022.1	2784.3	**3860.9**	3544.4	2370.0	3071.6	93.75	719.3
	Centipede	1814.1	3322.7	2750.7	5681.4	3833.2	**6322.7**	5484.1	162.2	1206.8
	Demon Attack	825.5	11523.0	4691.0	14140.9	6381.5	9486.8	**51045.9**	73.8	113.6
	Phoenix	427.6	10954.9	3071.0	14579.8	10797.3	9010.6	**22873.9**	0.0	8073.4
	Mean Improvement	0.42	1.00	0.69	1.36	1.02	1.11	**2.06**	0.02	0.29
	Median Improvement	0.55	1.00	0.83	1.28	1.15	0.82	**1.65**	0.01	0.24
Maze	Alien	152.9	695.0	641.5	**954.8**	722.8	703.6	633.6	108.1	294.1
	Amidar	25.5	109.7	84.2	90.2	**121.8**	70.8	69.7	0.0	5.2
	Bank Heist	178.8	246.1	244.5	**304.9**	280.1	225.1	261.4	0.0	7.3
	Ms Pacman	550.0	1281.4	1172.8	**1459.7**	1011.1	1122.6	809.2	147.6	448.9
	Wizard Of Wor	163.8	1033.1	928.8	985.0	**1246.1**	654.4	263.5	100.0	9.4
	Mean Improvement	0.35	1.00	0.90	**1.11**	1.06	0.82	0.70	0.07	0.17
	Median Improvement	0.23	1.00	0.92	**1.14**	1.11	0.88	0.64	0.10	0.05
Overall	Mean Improvement	0.39	1.00	0.79	1.23	1.04	0.96	**1.38**	0.05	0.23
	Median Improvement	0.33	1.00	0.91	**1.25**	1.12	0.85	1.04	0.02	0.16

- How does our proposed framework compare to alternative pretraining and online RL approaches with *limited* online interaction from the target task?
- How do the individual components of our framework influence its success?

Experimental setup. We base our architecture and backbone learning algorithm on EfficientZero (Ye et al., 2021) and focus our efforts on the pretraining and finetuning aspects of our problem setting. We consider EfficientZero with two different network sizes to better position our results: *(i)* the same network architecture as in the original EfficientZero implementation which we simply refer to as **EfficientZero**, and *(ii)* a larger variant with 4 times more parameters in the representation network (denoted **EfficientZero-L**). We use the EfficientZero-L variant as the default network for our framework through our experiments, unless stated otherwise. However, we find that our EfficientZero baseline generally does not benefit from a larger architecture, and we thus include both variants for a fair comparison. We experiment with cross-task transfer on three subsets of tasks: tasks that share *similar* game mechanics (for which we consider two ***Shooter*** and ***Maze*** categories), and tasks that have no discernible properties in common (referred to as ***Diverse***). We measure performance on individual Atari games by absolute scores, and also provide aggregate results as measured by mean and median scores across games, normalized by human performance or EfficientZero performance at 100k environment steps. All of our results are averaged across 5 random seeds (See Appendix D for more details). We also include offline data preparation procedure in Appendix F.

Baselines. We compare our method against **7** prior methods for online RL that represent the state-of-the-art on the Atari100k benchmark (including EfficientZero), as well as a multi-task behavior cloning policy trained on the full pretraining dataset, and a set of ablations that include EfficientZero with several different model sizes and pretraining/finetuning schemes. The former baselines serve to position our results with respect to the state-of-the-art, and the latter baselines and ablations serve to shed light on the key ingredients for successful multi-task pretraining and finetuning.

4.1 Results & Discussion

We introduce our results in the context of each of our three questions, and discuss our main findings.

How does our proposed framework compare to alternative pretraining and online RL approaches with limited *online interaction from the target task?*

Tasks that share *similar* game mechanics. We first investigate the feasibility of finetuning models that are pretrained on games with *similar* mechanics. We select 5 shooter games and 5 maze games for this experiment. Results for our method, baselines, and a set of ablations on the Atari100k benchmark are shown in Table 1. For completeness, we also provide learning curves in Figure 11 as well as an aggregate curve across 5 seeds of all 10 games normalized by EfficientZero's performance at 100K environment steps in Figure 1. We find that pretraining improves sample-efficiency substantially

Table 2. **Scores on the Atari 100k benchmark (diverse tasks)** The reported 5 XTRA results are from finetuning the same set of pretrained model parameters with the same 8 pretrained offline tasks. All numbers are computed for 5 seeds each with 32 evaluation episodes. Our result is highlighted. All other results are adopted from EfficientZero (Ye et al., 2021). CURL^{ft} is CURL by Srinivas et al. (2020) under the same offline pretraining + online finetuning setting as XTRA.

Game	XTRA (Ours)	EfficientZero	CURL^{ft}	CURL	Random	Human	SimPLe	OTRainbow	DrQ	SPR	MuZero
Assault	**1742.2**	1263.1	588.6	600.6	222.4	742.0	527.2	351.9	452.4	571.0	500.1
BattleZone	14631.25	13871.2	16450.0	14870.0	2360.0	37187.5	5184.4	4060.6	12954.0	**16651.0**	7687.5
Hero	**10631.8**	9315.9	6294.5	6279.3	1027.0	30826.4	2656.6	6458.8	3736.3	7019.2	3095.0
Krull	**7735.8**	5663.3	3472.8	4229.6	1598.0	2665.5	4539.9	3277.9	4018.1	3688.9	4890.8
Seaquest	749.5	1100.2	385.5	384.5	68.4	42054.7	683.3	286.9	301.2	583.1	208.0
Normed Mean	**1.87**	1.29	0.60	0.75	0.0	1.0	0.70	0.41	0.62	0.65	0.77
Normed Median	0.35	0.33	0.40	0.36	0.0	1.0	0.08	0.18	0.30	**0.41**	0.15

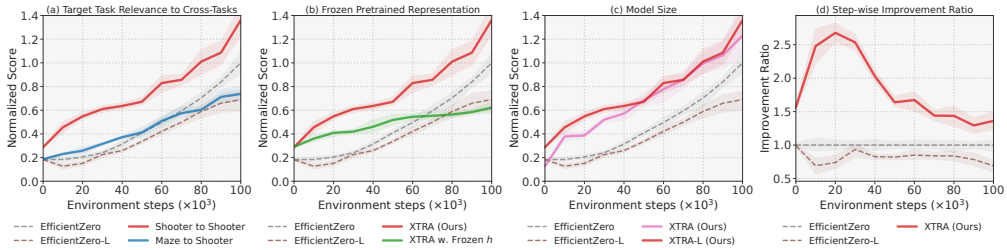

Figure 6. **(a) Effectiveness of Task Relavance, (b) Frozen Representation, (c) Model Size, and (d) Environment Steps**. We visualize model performance on aggregated scores (5 seeds) from 5 shooter games.

across most tasks, improving mean and median performance of EfficientZero by $\mathbf{23}\%$ and $\mathbf{25}\%$, respectively, overall. Interestingly, XTRA also had a notable zero-shot ability compared to a multi-game Behavioral Cloning baseline that is trained on the same offline dataset. We also consider three ablations: *(1)* **XTRA without cross-task:** a variant of our method that naively finetunes the pretrained model without any additional offline data from pretraining tasks during finetuning, *(2)* **XTRA without pretraining:** a variant that uses our concurrent cross-task learning (*i.e., leverages offline data during finetuning*) but is initialized with random parameters (no pretraining), and finally *(3)* **XTRA without task weights:** a variant that uses constant weights of 1 for all task loss terms during finetuning. We find that XTRA achieves extremely high performance on 2 games (DemonAttack and Phoenix) without dynamic task weights, improving over EfficientZero by as much as $\mathbf{343}\%$ on DemonAttack. However, its median performance is overall low compared to our default variant that uses dynamic weights. We conjecture that this is because some (combinations of) games are more susceptible to gradient conflicts than others. We also include offline pretraining + offline finetuning Behavioral Cloning baseline to compare with XTRA's performance in Table 1. See Appendix J for details.

Tasks with *diverse* game mechanics. We now consider a more diverse set of pretraining and target games that have no discernible properties in common. Specifically, we use the following tasks for pretraining: Carnival, Centipede, Phoenix, Pooyan, Riverraid, VideoPinball, WizardOfWor, and YarsRevenge, and evaluate our method on 5 tasks from Atari100k. Results are shown in Table 2. We find that XTRA advances the state-of-the-art in a majority of tasks on the Atari100k benchmark, and achieve a mean human-normalized score of $\mathbf{187}\%$ vs. $\mathbf{129}\%$ for the previous SOTA, EfficientZero. We also include a direct comparison to CURL Srinivas et al. (2020), a strong model-free RL baseline, under the same offline pretraining + online finetuning setting as XTRA. We implement CURL w/ pretraining + finetuning by following the experimental setup as for our model-based method: (1) we first pretrain on the same 8 offline tasks as our method, and then (2) finetune to the target task with online RL for 100k environment steps. We find that pretraining does not improve performance of the model-free method CURL as consistently as for our model-based framework, XTRA.

How do the individual components of our framework influence its success?

A deeper look at task relevance. While our previous experiments established that XTRA benefits from pretraining even when games are markedly different, we now seek to better quantify the importance of task relevance. We compare the online finetuning performance of XTRA in two different settings: *(1)* pretraining on 4 *shooter* games and finetuning to 5 new *shooter* games, and *(2)* pretraining on 4 *maze* games and finetuning to the same 5 *shooter* games. Aggregate results across all 5 target tasks are shown in Figure 6 (a). Unsurprisingly, we observe that offline pretraining and

concurrently learning from other shooter games significantly benefit the online target shooter games through training, with particularly large gains early in training. On the contrary, pretraining on maze games and finetuning to shooter games show similar performance compared to EfficientZero trained from scratch. This result indicates that *(1)* selecting pretraining tasks that are relevant to the target task is key to benefit from pretraining, and *(2)* in the extreme case where there are *no* pretraining tasks relevant to the target task, finetuning with XTRA generally does not harm the online RL performance since it can automatically assign small weights to the pretraining tasks.

Which components transfer in model-based RL? Next, we investigate which model component(s) are important to the success of cross-task transfer. We answer this question by only transferring a subset of the different model components – representation h, dynamics function g, and prediction head f – to the online finetuning stage and simply using a random initialization for the remaining components. Results are shown in Figure 7. Interestingly, we find that only transferring the pretrained representation h to the online RL stage only improves slightly over learning from scratch, especially in the early stages of online RL. In comparison, loading both the pretrained representation *and* dynamics function accounts for the majority of the gains in XTRA, whereas loading the prediction heads has no significant impact on sample-efficiency (but matters for zero-shot performance). We conjecture that this is because learning a good dynamics function is relatively more difficult from few samples than learning a *task-specific* visual representation, and that the prediction head accounts for only a small amount of the overall parameters in the model. Finally, we hypothesize that the visual representation learned during pretraining will be susceptible to distribution shifts as it is transferred to an unseen target task. To verify this hypothesis, we consider an additional experiment where we transfer all components to new tasks, but *freeze* the representation h during finetuning, *i.e.*, it remains fixed. Results for this experiment are shown in Figure 6 (b). We find that, although this variant of our framework improves over training from scratch in the early stages of training, the frozen representation eventually hinders the model from converging to a good model, which is consistent with observations made in (supervised) imitation learning (Parisi et al., 2022).

Scaling model size. In this experiment, we investigate whether XTRA benefits from larger model sizes. Since dynamics network g and prediction network f are used in MCTS search, increasing the parameter counts for these two networks would increase inference/training time complexity significantly. However, increasing the size of the representation network h has a relatively small impact on overall inference/training time (see Figure 3 for reference). We compare the performance of our method and EfficientZero trained from scratch with each of our two model sizes, the original EfficientZero architecture and a larger variant (denoted EfficientZero-**L**); results are shown in Figure 6 (c). We find that our default, larger variant of XTRA (denoted XTRA-L in the figure) is slightly better than the smaller model size. In comparison, EfficientZero-L, performs significantly worse than the smaller variant of EfficientZero.

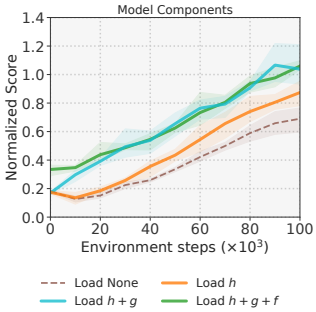

Figure 7. **Effectiveness of model components.** The aggregated scores from 5 shooter games by loading parameters of different pretrained model components. Here, h, g, and f denote the representation, dynamics, and prediction networks respectively.

Relative improvement vs. environment steps. Finally, we visualize the average improvement over EfficientZero throughout training in Figure 6 (d). The curve indicates that XTRA is particularly useful in the early stages of training, *i.e.*, in an extremely limited data setting. We therefore envision that cross-task pretraining could benefit many real-world applications of RL, where environment interactions are typically constrained due to physical constraints.

When can we empirically expect finetuning to be successful?

From Table 1, 2, we expect cross-task transfer with model-based RL is feasible, and Figure 6 (a) shows our XTRA framework benefits online finetuning when it is relevant to the pretrained tasks. We observe both representation, dynamics networks contribute to the successful transfer from Figure 7.

5 Related Work

Pretrained representations are widely used to improve downstream performance in learning tasks with limited data or resources available, and have been adopted across a multitude of areas such

as computer vision (Girshick et al., 2014; Doersch et al., 2015; He et al., 2020), natural language processing (Devlin et al., 2019; Brown et al., 2020), and audio (van den Oord et al., 2018). By first learning a good representation on a large dataset, the representation can quickly be finetuned with, *e.g.*, supervised learning on a small labelled dataset to solve a given task (Pan & Yang, 2010). For example, He et al. (2020) show that contrastive pretraining on a large, unlabelled dataset learns good features for ImageNet classification, and Brown et al. (2020) show that a generative model trained on large-scale natural language data can be used to solve unseen tasks given only a few examples. While this is a common paradigm for problems that can be cast as (self-)supervised learning problems, it has seen comparably little adoption in RL literature. This discrepancy is, in part, attributed to optimization challenges in RL (Bodnar et al., 2020; Hansen et al., 2021b; Xiao et al., 2022; Wang et al., 2022), as well as a lack of large-scale datasets that capture both the visual, temporal, and control-relevant (actions, rewards) properties of RL. In this work, we show that – despite these challenges – modern model-based RL algorithms can still benefit substantially from pretraining on multi-task datasets, but require a more careful treatment during finetuning.

Sample-efficient RL. Improving the sample-efficiency of visual RL algorithms is a long-standing problem and has been approached from many – largely orthogonal – perspectives, including representation learning (Kulkarni et al., 2019; Yarats et al., 2019; Srinivas et al., 2020; Schwarzer et al., 2021), data augmentation (Laskin et al., 2020; Kostrikov et al., 2021; Hansen et al., 2021b), bootstrapping from demonstrations (Zhan et al., 2020) or offline datasets (Wang et al., 2022; Zheng et al., 2022; Baker et al., 2022), using pretrained visual representations for model-free RL (Shah & Kumar, 2021; Xiao et al., 2022), and model-based RL (Ha & Schmidhuber, 2018; Finn & Levine, 2017; Nair et al., 2018; Hafner et al., 2019b; Kaiser et al., 2020; Schrittwieser et al., 2020; Hafner et al., 2021; Ye et al., 2021; Hansen et al., 2022; Seo et al., 2022). We choose to focus our efforts on sample-efficiency from the perspective of pretraining in a model-based context, *i.e.*, jointly learning perception *and* dynamics. Several prior works consider these problems independently from each other: Xiao et al. (2022) shows that model-free policies can be trained with a frozen pretrained visual backbone, and Seo et al. (2022) shows that learning a world model on top of features from a visual backbone pretrained with video prediction can improve model learning. Our work differs from prior work in that we show it is possible to pretrain *and* finetune both the representation *and* the dynamics using model-based RL.

Finetuning in RL. Gradient-based finetuning is a well-studied technique for adaptation in (predominantly model-free) RL, and has been used to adapt to either changes in visuals or dynamics (Mishra et al., 2017; Yen-Chen et al., 2019; Duan et al., 2016; Julian et al., 2020; Hansen et al., 2021a; Bodnar et al., 2020), or task specification (Xie & Finn, 2021; Walke et al., 2022). For example, Julian et al. (2020) shows that a model-free policy for robotic manipulation can adapt to changes in lighting and object shape by finetuning via rewards on a mixture of data from the new and old environment, and recover original performance in less than 800 trials. Similarly, Hansen et al. (2021a) shows that model-free policies can (to some extent) also adapt to small domain shifts by self-supervised finetuning within a single episode. Other works show that pretraining with offline RL on a dataset from a specific task improve sample-efficiency during online finetuning on the same task (Zheng et al., 2022; Wang et al., 2022). Finally, Lee et al. (2022) shows that offline multi-task RL pretraining via sequence modelling can improve offline finetuning on data from unseen tasks. Our approach is most similar to Julian et al. (2020) in that we finetune via rewards on a mixture of datasets. However, our problem setting is fundamentally different: we investigate whether *multi-task* pretraining can improve online RL on an *unseen* task across *multiple* axes of variation.

6 Conclusion

In this paper, we propose Model-Based **Cross**-Task **Tra**nsfer (**XTRA**), a framework for sample-efficient online RL with scalable pretraining and finetuning of learned world models using extra, auxiliary data from other tasks. We find that XTRA improves sample-efficiency substantially across most tasks, improving mean and median performance of EfficientZero by 23% and 25%, respectively, overall. We hope our analysis and findings on the feasibility of cross-task transfer with model-based RL can greatly benefit future studies in this direction.

Reproducibility Statement. We base all experiments on the publicly available Atari100k benchmark, and provide extensive implementation details in the appendices, including detailed network architecture and hyper-parameters. *We are committed to releasing our code publicly.*

REFERENCES

Bruce D. Abramson. *The Expected-Outcome Model of Two-Player Games*. PhD thesis, 1987. AAI8827528.

Jean-Baptiste Alayrac, Jeff Donahue, Pauline Luc, Antoine Miech, Iain Barr, Yana Hasson, Karel Lenc, Arthur Mensch, Katie Millican, Malcolm Reynolds, et al. Flamingo: a visual language model for few-shot learning. *arXiv preprint arXiv:2204.14198*, 2022.

Adrià Puigdomènech Badia, Bilal Piot, Steven Kapturowski, Pablo Sprechmann, Alex Vitvitskyi, Daniel Guo, and Charles Blundell. Agent57: Outperforming the atari human benchmark. *ArXiv*, abs/2003.13350, 2020.

Bowen Baker, Ilge Akkaya, Peter Zhokhov, Joost Huizinga, Jie Tang, Adrien Ecoffet, Brandon Houghton, Raul Sampedro, and Jeff Clune. Video pretraining (vpt): Learning to act by watching unlabeled online videos. *ArXiv*, abs/2206.11795, 2022.

Marc G. Bellemare, Yavar Naddaf, Joel Veness, and Michael Bowling. The arcade learning environment: An evaluation platform for general agents (extended abstract). In *IJCAI*, 2013.

Richard Bellman. A markovian decision process. *Journal of Mathematics and Mechanics*, 6(5): 679–684, 1957.

Christopher Berner, Greg Brockman, Brooke Chan, Vicki Cheung, Przemyslaw Debiak, Christy Dennison, David Farhi, Quirin Fischer, Shariq Hashme, Christopher Hesse, Rafal Józefowicz, Scott Gray, Catherine Olsson, Jakub W. Pachocki, Michael Petrov, Henrique Pondé de Oliveira Pinto, Jonathan Raiman, Tim Salimans, Jeremy Schlatter, Jonas Schneider, Szymon Sidor, Ilya Sutskever, Jie Tang, Filip Wolski, and Susan Zhang. Dota 2 with large scale deep reinforcement learning. *ArXiv*, abs/1912.06680, 2019.

Cristian Bodnar, Karol Hausman, Gabriel Dulac-Arnold, and Rico Jonschkowski. A geometric perspective on self-supervised policy adaptation. *ArXiv*, abs/2011.07318, 2020.

Tom B. Brown, Benjamin Mann, Nick Ryder, Melanie Subbiah, Jared Kaplan, Prafulla Dhariwal, Arvind Neelakantan, Pranav Shyam, Girish Sastry, Amanda Askell, Sandhini Agarwal, Ariel Herbert-Voss, Gretchen Krueger, T. J. Henighan, Rewon Child, Aditya Ramesh, Daniel M. Ziegler, Jeff Wu, Clemens Winter, Christopher Hesse, Mark Chen, Eric Sigler, Mateusz Litwin, Scott Gray, Benjamin Chess, Jack Clark, Christopher Berner, Sam McCandlish, Alec Radford, Ilya Sutskever, and Dario Amodei. Language models are few-shot learners. *ArXiv*, abs/2005.14165, 2020.

Aakanksha Chowdhery, Sharan Narang, Jacob Devlin, Maarten Bosma, Gaurav Mishra, Adam Roberts, Paul Barham, Hyung Won Chung, Charles Sutton, Sebastian Gehrmann, et al. Palm: Scaling language modeling with pathways. *arXiv preprint arXiv:2204.02311*, 2022.

Karl Cobbe, Christopher Hesse, Jacob Hilton, and John Schulman. Leveraging procedural generation to benchmark reinforcement learning. *ArXiv*, abs/1912.01588, 2020.

Rémi Coulom. Efficient selectivity and backup operators in monte-carlo tree search. In *International conference on computers and games*, pp. 72–83. Springer, 2006.

Jacob Devlin, Ming-Wei Chang, Kenton Lee, and Kristina Toutanova. Bert: Pre-training of deep bidirectional transformers for language understanding. *ArXiv*, abs/1810.04805, 2019.

Carl Doersch, Abhinav Kumar Gupta, and Alexei A. Efros. Unsupervised visual representation learning by context prediction. *2015 IEEE International Conference on Computer Vision (ICCV)*, pp. 1422–1430, 2015.

Yan Duan, John Schulman, Xi Chen, Peter L. Bartlett, Ilya Sutskever, and P. Abbeel. Rl2: Fast reinforcement learning via slow reinforcement learning. *ArXiv*, abs/1611.02779, 2016.

Rachit Dubey, Pulkit Agrawal, Deepak Pathak, Thomas L. Griffiths, and Alexei A. Efros. Investigating human priors for playing video games. In *ICML*, 2018.

Chelsea Finn and Sergey Levine. Deep visual foresight for planning robot motion. *2017 IEEE International Conference on Robotics and Automation (ICRA)*, pp. 2786–2793, 2017.

Ross B. Girshick, Jeff Donahue, Trevor Darrell, and Jitendra Malik. Rich feature hierarchies for accurate object detection and semantic segmentation. *2014 IEEE Conference on Computer Vision and Pattern Recognition*, pp. 580–587, 2014.

David Ha and Jürgen Schmidhuber. Recurrent world models facilitate policy evolution. *Advances in neural information processing systems*, 31, 2018.

Danijar Hafner, Timothy Lillicrap, Jimmy Ba, and Mohammad Norouzi. Dream to control: Learning behaviors by latent imagination. *arXiv preprint arXiv:1912.01603*, 2019a.

Danijar Hafner, Timothy P. Lillicrap, Ian S. Fischer, Ruben Villegas, David R Ha, Honglak Lee, and James Davidson. Learning latent dynamics for planning from pixels. *ArXiv*, abs/1811.04551, 2019b.

Danijar Hafner, Timothy P. Lillicrap, Mohammad Norouzi, and Jimmy Ba. Mastering atari with discrete world models. *ArXiv*, abs/2010.02193, 2021.

Nicklas Hansen, Rishabh Jangir, Yu Sun, Guillem Alenyà, Pieter Abbeel, Alexei A. Efros, Lerrel Pinto, and Xiaolong Wang. Self-supervised policy adaptation during deployment. In *International Conference on Learning Representations (ICLR)*, 2021a.

Nicklas Hansen, Hao Su, and Xiaolong Wang. Stabilizing deep q-learning with convnets and vision transformers under data augmentation. In *NeurIPS*, 2021b.

Nicklas Hansen, Xiaolong Wang, and Hao Su. Temporal difference learning for model predictive control. In *ICML*, 2022.

Kaiming He, Haoqi Fan, Yuxin Wu, Saining Xie, and Ross B. Girshick. Momentum contrast for unsupervised visual representation learning. *2020 IEEE/CVF Conference on Computer Vision and Pattern Recognition (CVPR)*, pp. 9726–9735, 2020.

Ryan C. Julian, Benjamin Swanson, Gaurav S. Sukhatme, Sergey Levine, Chelsea Finn, and Karol Hausman. Efficient adaptation for end-to-end vision-based robotic manipulation. *ArXiv*, abs/2004.10190, 2020.

Leslie Pack Kaelbling, Michael L. Littman, and Anthony R. Cassandra. Planning and acting in partially observable stochastic domains. *Artificial Intelligence*, 1998.

Lukasz Kaiser, Mohammad Babaeizadeh, Piotr Milos, Blazej Osinski, Roy H. Campbell, K. Czechowski, D. Erhan, Chelsea Finn, Piotr Kozakowski, Sergey Levine, Ryan Sepassi, G. Tucker, and Henryk Michalewski. Model-based reinforcement learning for atari. *ArXiv*, abs/1903.00374, 2020.

Ilya Kostrikov, Denis Yarats, and Rob Fergus. Image augmentation is all you need: Regularizing deep reinforcement learning from pixels. *ArXiv*, abs/2004.13649, 2021.

Tejas D. Kulkarni, Ankush Gupta, Catalin Ionescu, Sebastian Borgeaud, Malcolm Reynolds, Andrew Zisserman, and Volodymyr Mnih. Unsupervised learning of object keypoints for perception and control. *ArXiv*, abs/1906.11883, 2019.

Aviral Kumar, Aurick Zhou, G. Tucker, and Sergey Levine. Conservative q-learning for offline reinforcement learning. *ArXiv*, abs/2006.04779, 2020.

Michael Laskin, Kimin Lee, Adam Stooke, Lerrel Pinto, P. Abbeel, and A. Srinivas. Reinforcement learning with augmented data. *ArXiv*, abs/2004.14990, 2020.

Kuang-Huei Lee, Ofir Nachum, Mengjiao Yang, L. Y. Lee, Daniel Freeman, Winnie Xu, Sergio Guadarrama, Ian S. Fischer, Eric Jang, Henryk Michalewski, and Igor Mordatch. Multi-game decision transformers. *ArXiv*, abs/2205.15241, 2022.

Chunyuan Li, Haotian Liu, Liunian Harold Li, Pengchuan Zhang, Jyoti Aneja, Jianwei Yang, Ping Jin, Yong Jae Lee, Houdong Hu, Zicheng Liu, et al. Elevater: A benchmark and toolkit for evaluating language-augmented visual models. *arXiv preprint arXiv:2204.08790*, 2022.

Nikhil Mishra, Mostafa Rohaninejad, Xi Chen, and P. Abbeel. Meta-learning with temporal convolutions. *ArXiv*, abs/1707.03141, 2017.

Volodymyr Mnih, Koray Kavukcuoglu, David Silver, Alex Graves, Ioannis Antonoglou, Daan Wierstra, and Martin Riedmiller. Playing atari with deep reinforcement learning. *arXiv preprint arXiv:1312.5602*, 2013.

Ashvin Nair, Vitchyr H. Pong, Murtaza Dalal, Shikhar Bahl, Steven Lin, and Sergey Levine. Visual reinforcement learning with imagined goals. In *NeurIPS*, 2018.

Sinno Jialin Pan and Qiang Yang. A survey on transfer learning. *IEEE Transactions on Knowledge and Data Engineering*, 22:1345–1359, 2010.

Simone Parisi, Aravind Rajeswaran, Senthil Purushwalkam, and Abhinav Kumar Gupta. The unsurprising effectiveness of pre-trained vision models for control. In *ICML*, 2022.

Emilio Parisotto, Lei Jimmy Ba, and Ruslan Salakhutdinov. Actor-mimic: Deep multitask and transfer reinforcement learning. In *ICLR (Poster)*, 2016.

Alec Radford, Jong Wook Kim, Chris Hallacy, Aditya Ramesh, Gabriel Goh, Sandhini Agarwal, Girish Sastry, Amanda Askell, Pamela Mishkin, Jack Clark, et al. Learning transferable visual models from natural language supervision. In *International Conference on Machine Learning*, pp. 8748–8763, 2021.

Scott Reed, Konrad Zolna, Emilio Parisotto, Sergio Gomez Colmenarejo, Alexander Novikov, Gabriel Barth-Maron, Mai Gimenez, Yury Sulsky, Jackie Kay, Jost Tobias Springenberg, Tom Eccles, Jake Bruce, Ali Razavi, Ashley D. Edwards, Nicolas Manfred Otto Heess, Yutian Chen, Raia Hadsell, Oriol Vinyals, Mahyar Bordbar, and Nando de Freitas. A generalist agent. *ArXiv*, abs/2205.06175, 2022.

Andrei A Rusu, Sergio Gomez Colmenarejo, Çaglar Gülçehre, Guillaume Desjardins, James Kirkpatrick, Razvan Pascanu, Volodymyr Mnih, Koray Kavukcuoglu, and Raia Hadsell. Policy distillation. In *ICLR (Poster)*, 2016.

Julian Schrittwieser, Ioannis Antonoglou, Thomas Hubert, Karen Simonyan, L. Sifre, Simon Schmitt, Arthur Guez, Edward Lockhart, Demis Hassabis, Thore Graepel, Timothy P. Lillicrap, and David Silver. Mastering atari, go, chess and shogi by planning with a learned model. *Nature*, 2020.

Julian Schrittwieser, Thomas K Hubert, Amol Mandhane, Mohammadamin Barekatain, Ioannis Antonoglou, and David Silver. Online and offline reinforcement learning by planning with a learned model. In A. Beygelzimer, Y. Dauphin, P. Liang, and J. Wortman Vaughan (eds.), *Advances in Neural Information Processing Systems*, 2021. URL https://openreview.net/forum?id=HKtsGW-lNbw.

Max Schwarzer, Ankesh Anand, Rishab Goel, R. Devon Hjelm, Aaron C. Courville, and Philip Bachman. Data-efficient reinforcement learning with self-predictive representations. In *ICLR*, 2021.

Younggyo Seo, Kimin Lee, Stephen James, and P. Abbeel. Reinforcement learning with action-free pre-training from videos. In *ICML*, 2022.

Rutav Shah and Vikash Kumar. Rrl: Resnet as representation for reinforcement learning. *ArXiv*, abs/2107.03380, 2021.

David Silver, Aja Huang, Christopher Maddison, Arthur Guez, Laurent Sifre, George Driessche, Julian Schrittwieser, Ioannis Antonoglou, Veda Panneershelvam, Marc Lanctot, Sander Dieleman, Dominik Grewe, John Nham, Nal Kalchbrenner, Ilya Sutskever, Timothy Lillicrap, Madeleine Leach, Koray Kavukcuoglu, Thore Graepel, and Demis Hassabis. Mastering the game of go with deep neural networks and tree search. *Nature*, 529:484–489, 01 2016. doi: 10.1038/nature16961.

A. Srinivas, Michael Laskin, and P. Abbeel. Curl: Contrastive unsupervised representations for reinforcement learning. In *ICML*, 2020.

Aäron van den Oord, Yazhe Li, and Oriol Vinyals. Representation learning with contrastive predictive coding. *ArXiv*, abs/1807.03748, 2018.

Homer Walke, Jonathan Yang, Albert Yu, Aviral Kumar, Jedrzej Orbik, Avi Singh, and Sergey Levine. Don't start from scratch: Leveraging prior data to automate robotic reinforcement learning. *ArXiv*, abs/2207.04703, 2022.

Che Wang, Xufang Luo, Keith W. Ross, and Dongsheng Li. Vrl3: A data-driven framework for visual deep reinforcement learning. *ArXiv*, abs/2202.10324, 2022.

Tete Xiao, Ilija Radosavovic, Trevor Darrell, and Jitendra Malik. Masked visual pre-training for motor control. *ArXiv*, abs/2203.06173, 2022.

Annie Xie and Chelsea Finn. Lifelong robotic reinforcement learning by retaining experiences. *ArXiv*, abs/2109.09180, 2021.

Denis Yarats, Amy Zhang, Ilya Kostrikov, Brandon Amos, Joelle Pineau, and Rob Fergus. Improving sample efficiency in model-free reinforcement learning from images. 2019.

Weirui Ye, Shaohuai Liu, Thanard Kurutach, P. Abbeel, and Yang Gao. Mastering atari games with limited data. In *NeurIPS*, 2021.

Lin Yen-Chen, Maria Bauza, and Phillip Isola. Experience-embedded visual foresight. In *Conference on Robot Learning*, 2019.

Tianhe Yu, Saurabh Kumar, Abhishek Gupta, Sergey Levine, Karol Hausman, and Chelsea Finn. Gradient surgery for multi-task learning. *Advances in Neural Information Processing Systems*, 33: 5824–5836, 2020.

Albert Zhan, Philip Zhao, Lerrel Pinto, P. Abbeel, and Michael Laskin. A framework for efficient robotic manipulation. *ArXiv*, abs/2012.07975, 2020.

Qinqing Zheng, Amy Zhang, and Aditya Grover. Online decision transformer. In *ICML*, 2022.

A APPENDIX: XTRA/EFFICIENTZERO OBJECTIVES

XTRA uses the same learning objective as EfficientZero during both offline pretraining and online finetuning, except the quantity targets are predicted by the teacher model during distillation and concurrent learning for pretrained games instead of Muzero Reanalysis procedure.

Here, we explain the objectives of EfficientZero (Ye et al., 2021) and its predecessor MuZero (Schrittwieser et al., 2020). To warrant the latent dynamics that can mirror the true states of the environment, MuZero is trained to predict three necessary quantities directly relevant for planning: (1) the policy target π obtained from visit count distribution of the MCTS (2) immediate reward u from environment (3) bootstrapped value target z where $z = \sum_{i=0}^{k-1} \gamma^i u^i + \gamma^k v_{t+k}$. On top of MuZero, EfficientZero adds a self-supervised consistency loss term, and predicts sum of environment rewards from next k steps, $\sum_{i=0}^{k-1} \gamma^i u^i$, instead of single-step reward. We refer reader to the original manuscript for implementation details (Ye et al., 2021). We present the learning objective for EfficientZero at time step t with k unroll steps:

$$\mathcal{L}_t^{\text{ez}}(\theta) = \sum_{k=0}^{K} \underbrace{\|\mathcal{L}^r(u_{t+k}, \hat{r}_t^k)\|_2^2}_{\text{reward}} + \lambda_1 \underbrace{\|\mathcal{L}^p(\pi_{t+k}, \hat{p}_t^k)\|_2^2}_{\text{policy}} + \lambda_2 \underbrace{\|\mathcal{L}^v(z_{t+k}, \hat{v}_t^k)\|_2^2}_{\text{value}} + \lambda_3 \underbrace{\|\mathcal{L}^s(s_{t+1}, \hat{s}_{t+1})\|_2^2}_{\text{consistency}} + c||\theta|| \tag{3}$$

B APPENDIX: TASK WEIGHTS COMPUTATION

Within the N-steps update, we maintain a task-specific counter s^i and update the counter by Δs_n^i at each step n as follows:

$$\Delta s_n^i = \begin{cases} 1, & \text{if } \ \text{Sim}(\tilde{\mathcal{M}}^i, \mathcal{M}) > 0.1 \\ 0, & \text{otherwise.} \end{cases}$$
$$s^i = s^i + \Delta s_n^i \tag{4}$$

After N steps, the new task weights η^i can be reset by $\eta^i = \frac{s^i}{N}$, and be adopted in our online adaptation objective in Equation 1. In practice, we start task weights update at 10k steps to ensure enough data from the online target task is collected. All task weights are initialized as 1 for the first 10k steps, and reset at the beginning of each every T-cycle.

Figure 8 shows how task weights are adaptively adjusted by the model during 100k environment steps during online finetuning stage for 10 games reported in Figure 11. Figure 9 shows the adjustments of task weights for 5 games reported in Figure 12.

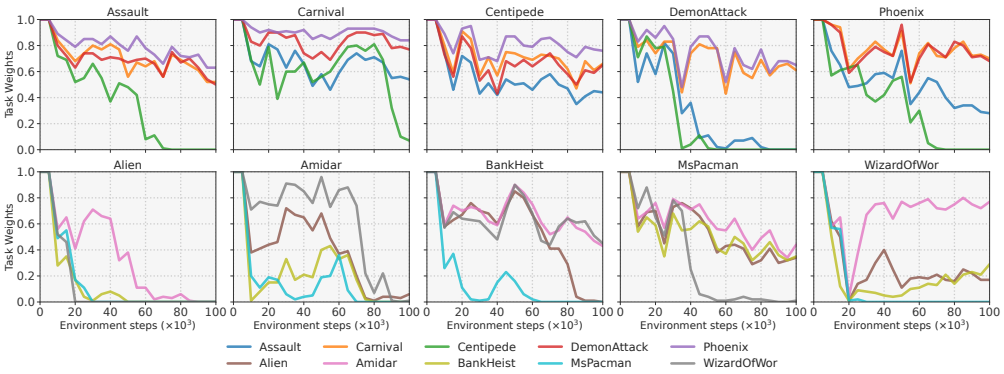

Figure 8. Task weights adaptively adjusted by the model as it progresses in online finetuning to the target task under *similar* task pretraining setting.

C APPENDIX: COMPARISON BETWEEN MULTI-GAME OFFLINE TRAINING AND DISTILLATION

In Figure 10, we present results from multi-game offline training and multi-game distillation for 4 games. The multi-game results are evaluated from a single set of model parameters trained with

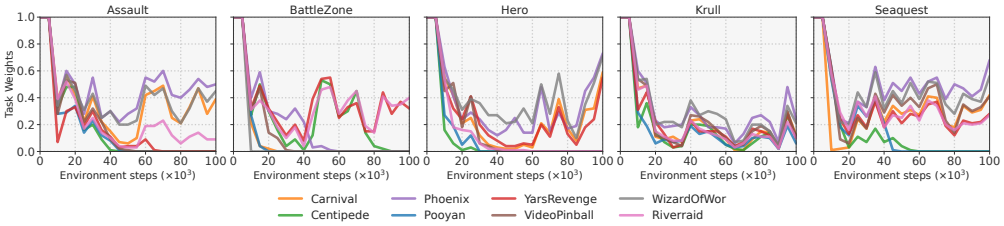

Figure 9. Task weights adaptively adjusted by the model as it progresses in online finetuning to the target task under *diverse* task pretraining setting.

all 4 games. While the model can easily learn each game individually (offline single game), it fails to learn 4 games simultaneously in the offline setting. On the opposite, our multi-game distillation successfully learns 4 games from teacher targets in multi-task fashion.

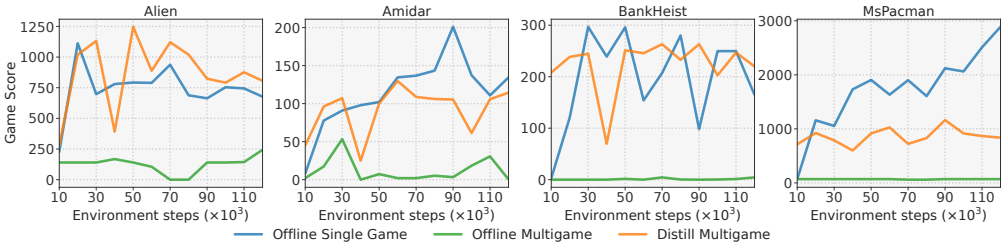

Figure 10. Comparison between Multi-Game Offline Training and Distillation

D Appendix: XTRA Game Scores for Table 1.

We report raw game scores from our XTRA stated in Table 1 for all 5 seeds we have run. We attach the mean, median, and standard deviation of game scores from 5 seeds of each individual game. We also list the random and human score from Badia et al. (2020), and calculate the Human Normalized Score based on the formula: $(\text{score}_{\text{agent}} - \text{score}_{\text{random}})/(\text{score}_{\text{human}} - \text{score}_{\text{random}})$. There is no random or human score available for Carnival, and therefore the aggregated Human Normalized Mean and Median Scores are calculated from the other 9 games. Details are in Table 3.

Table 3. Game score per seed and its aggregate results. Random and human scores are adopted from Badia et al. (2020).

Game	Game Score per Seed					Aggregated Metrics			References		Human Normed
	Seed 0	Seed 1	Seed 2	Seed 3	Seed 4	Mean	Median	Std	Random	Human	
Assault	1450.19	1356.53	1236.19	1215.12	1214.72	1294.55	1236.19	105.06	222.40	742.00	2.06
Carnival	3865.31	4867.50	4155.62	2601.88	3814.38	3860.94	3865.31	819.67	-	-	
Centipede	7596.38	6179.25	5380.41	5300.03	3950.88	5681.39	5380.41	1336.58	2090.90	12017.00	0.36
DemonAttack	10470.78	8051.25	27574.06	8117.81	16490.47	14140.88	10470.78	8258.35	152.10	1971.00	7.69
Phoenix	20875.94	10988.44	10521.88	15803.44	14709.06	14579.75	14709.06	4198.81	761.40	7242.60	2.13
Alien	569.69	807.50	814.06	1388.12	1194.38	954.75	814.06	329.77	227.80	7127.70	0.11
Amidar	93.00	104.34	76.47	97.38	79.59	90.16	93.00	11.84	5.80	1719.50	0.05
BankHeist	303.12	316.56	270.62	270.00	364.06	304.88	303.12	38.83	14.20	753.10	0.39
MsPacman	1109.69	1960.00	1865.94	1228.44	1134.38	1459.69	1228.44	417.48	307.30	6951.60	0.17
WizardOfWor	1275.00	687.50	1056.25	990.62	915.62	985.00	990.62	213.62	563.50	4756.50	0.10
Human Normed Mean											1.45
Human Normed Median											0.36

E Appendix: Additional Evaluation curves of XTRA on Atari 100k benchmark

For completeness, Figure 11 and 12 include evaluation curves of XTRA on the games for which we report final performance in Table 1 and 2.

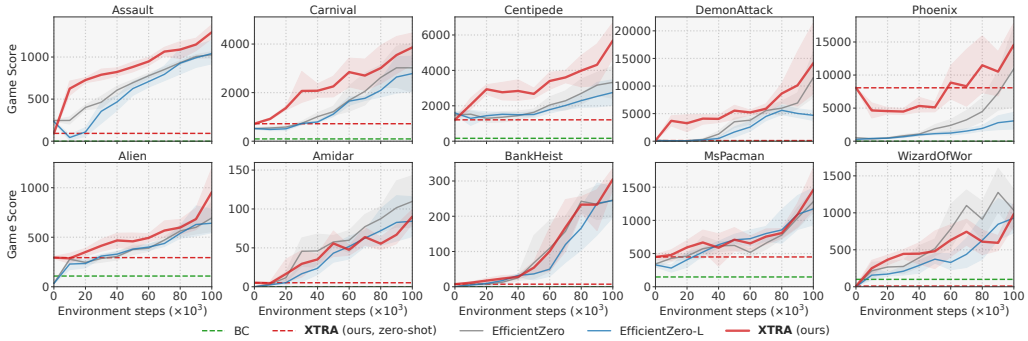

Figure 11. **Evaluation curves of our method (XTRA) and baselines over 100k environment steps.** Scores are aggregated across 5 seeds for each game; shaded area represents the 95% confidence interval.

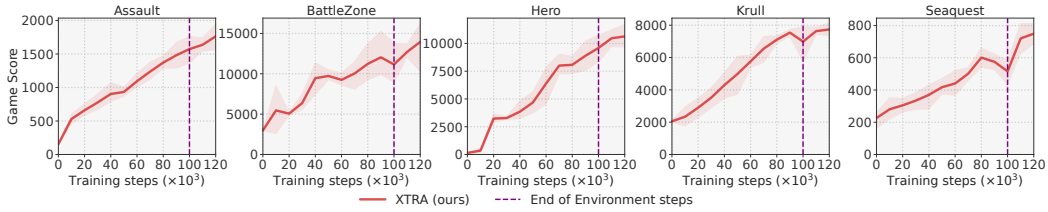

Figure 12. Evaluation curves of XTRA on Atari 100k benchmark

F Appendix: Offline Data Preparation

To train the model in offline multi-task pretraining stage, we use collected trajectories of EfficientZero Ye et al. (2021) from the Atari100k benchmark. For each pretraining game, we assume we can access model checkpoints obtained from 100k environment steps and 120k training steps, resulting in 12 model checkpoints. For each model checkpoint, we repeat the self-play procedure in EfficientZero Ye et al. (2021) to collect 64 trajectories.This translates to an average of 1M transitions per game, but varies depending on episode length – for example, this only results in 636k transitions for the game of Assault. Thus, we show that XTRA is effective even when pretraining data is suboptimal, allowing us to learn from very diverse data sources.

G Appendix: Hyper-parameters for XTRA and EfficientZero Model Architecture

We follow the EfficientZero's official architecture implementation to make straight comparison. For EfficientZero-L and XTRA, we increase number of convolutions layers from 1 to 4 to linearly scale up the size of representation networks.

The architecture of the **representation networks** is as follows:

- 1 convolution with stride 2 and 32 output planes, output resolution 48x48. (BN + ReLU)
- 1 residual block with 32 planes.
- 1 residual downsample block with stride 2 and 64 output planes, output resolution 24x24.
- 1 residual block with 64 planes.
- Average pooling with stride 2, output resolution 12x12. (BN + ReLU)
- 1 residual block with 64 planes.
- Average pooling with stride 2, output resolution 6x6. (BN + ReLU)
- 1 residual block with 64 planes.

, where the kernel size is 3×3 for all operations.

The architecture of the **dynamics networks** is as follows:

- Concatenate the input states and input actions into 65 planes.
- 1 convolution with stride 2 and 64 output planes. (BN)
- A residual link: add up the output and the input states. (ReLU)
- 1 residual block with 64 planes.

The architecture of the **reward prediction network** is as follows:

- 1 1x1convolution and 16 output planes. (BN + ReLU)
- Flatten.
- LSTM with 512 hidden size. (BN + ReLU)
- 1 fully connected layers and 32 output dimensions. (BN + ReLU)
- 1 fully connected layers and 601 output dimensions.

The architecture of the **value and policy prediction networks** is as follows:

- 1 residual block with 64 planes.
- 1 1x1convolution and 16 output planes. (BN + ReLU)
- Flatten.
- 1 fully connected layers and 32 output dimensions. (BN + ReLU)
- 1 fully connected layers and D output dimensions.

, where $D = 601$ in the value prediction network and $D = action\ space$ in the policy prediction network.

H APPENDIX: HYPER-PARAMETERS FOR ONLINE FINETUNING XTRA

In this paper, we adopted all hyper-parameters for EfficientZero to make straight comparison except training steps and reanalyzed policy ratio. In the original EfficientZero paper, EfficientZero trains the model for additional 20k steps after collecting 100k environment steps data and decay learning rate by 0.1. We set training steps to 120k as original EfficientZero setting for Table 2 to make direct and fair comparison to the reported number from EfficientZero paper. We set training steps to 100k to match exact 100k environment steps with no additional training for all other results reported in this paper for running both EfficientZero baselines (EfficientZero and EfficientZero-L) and our XTRA models.

Table 4. Hyper-parameters for Online Finetuning XTRA on Atari games

Parameter	Setting
Observation down-sampling	96×96
Frames stacked	4
Frames skip	4
Reward clipping	True
Terminal on loss of life	True
Max frames per episode	108K
Discount factor	0.997^4
Minibatch size	256
Optimizer	SGD
Optimizer: learning rate	0.2
Optimizer: momentum	0.9
Optimizer: weight decay (c)	0.0001
Learning rate schedule	$0.2 \rightarrow 0.02$
Max gradient norm	5
Priority exponent (α)	0.6
Priority correction (β)	$0.4 \rightarrow 1$
Training steps	100K/120K
Evaluation episodes	32
Min replay size for sampling	2000
Self-play network updating inerval	100
Target network updating interval	200
Unroll steps (l_{unroll})	5
TD steps (k)	5
Policy loss coefficient (λ_1)	1
Value loss coefficient (λ_2)	0.25
Self-supervised consistency loss coefficient (λ_3)	2
LSTM horizontal length (ζ)	5
Dirichlet noise ratio (ξ)	0.3
Number of simulations in MCTS (N_{sim})	50
Reanalyzed policy ratio	1.0

I APPENDIX: GAME INFORMATION

We provide information on games appeared in pretraining and finetuning for XTRA. The **Similar Task** column marks all the games used in Table 1 , and the two **Diverse Task** column mark all the games used in Table 2 for pretraining and finetuning the model. We define all the games in the following categories: Maze, Shooter, Tank, Adventure, and Ball Tracking.

In the Maze category, the actor is required to move horizontally or vertically to find a path to (1) pick up objectives to gain scores or special abilities, and (2) avoid being caught by moving enemies. In the Shooter category, the actor is required to shoot horizontally or vertically toward objectives, and at the same time avoid being shot by enemies. In the Tank category, the actor is required to move a fighting vehicle into any directions on a plane, shoot to the enemies appearing on the map and avoid being hit; it is worth mentioning that in this category, the visual observation appears in the First-Person Perspective (FPP), which is different from the visual observation from the shooter category, where the visual observation appears in Third-Person Perspective (TPP) with absolute positioning (e.g. the background is fixed). In the adventure category, the actor is required to perform a diverse set of skills which can differ from game to game; these skills often include shooting, hitting the enemies, solving mazes, and protecting targets, some of which can also be seen from other game categories. In the

Ball Tracking category, the actor is required to keep track of a moving ball, and hit it to prevent the ball from moving off the gaming area.

We also include attributes in terms of **scene continuity** and **action space**. A continuous scene represents that within the game, there will not be sudden changes of a visual observation possibly due to actor moving out of the current gaming zone, leveling up, etc. Action space refers to the number of actions that the actor is able to use for a game. The maximum action space for Atari games is 18.

Table 5. **Information on games relavant to Table 1 and Table 2.** In Table 1, we finetune the model to each game after pretraining it on the other games within the same category. In Table 2, we finetune the model to each game after pretraining it on all eight games.

Games	Similar Task (Pretrain & Fine Tune)	Diverse Task (Pretrain)	Diverse Task (Fine Tune)	Category	Scene Continuity	Action Space
Alien	✓			Maze		18
Amidar	✓			Maze	✓	10
Assault	✓		✓	Shooter	✓	7
Bank Heist	✓			Maze		18
Carnival	✓	✓		Shooter	✓	6
Centipede	✓	✓		Shooter	✓	18
DemonAttack	✓			Shooter	✓	6
MsPacman	✓			Maze		9
Phoenix	✓	✓		Shooter		8
WizardOfWor	✓	✓		Maze		10
BattleZone			✓	Tank	✓	18
Hero			✓	Adventure		18
Krull			✓	Adventure		18
Seaquest			✓	Shooter	✓	18
Pooyan		✓		Shooter		6
Riverraid		✓		Shooter	✓	18
VideoPinball		✓		Ball Tracking		9
YarsRevenge		✓		Shooter		18

J APPENDIX: BEHAVIORAL CLONING BASELINE

We use the representation + prediction network in XTRA for the behavioral cloning (BC) study. The BC (finetune) from Table 1 follows an offline pretraining + offline finetuning paradigm. The model is finetuned on offline data for the target task (also generated by the EfficientZero baseline). We find BC (finetune) underperforms the EfficientZero baseline. We also report zero-shot performance of the pretrained BC on their designated target tasks directly.

K APPENDIX: GAME VISUALIZATIONS

To better understand the feasibility of cross-task transfer, we show sample trajectory from our experiment games. Figure 13 and 14 include all games involved in Table 1 (tasks sharing similar game mechanics). Figure 15 include pretraining/finetuning games involved in Table 2 (tasks sharing diverse game mechanics) excluding ones that are shown in Figure 13 and Figure 14.

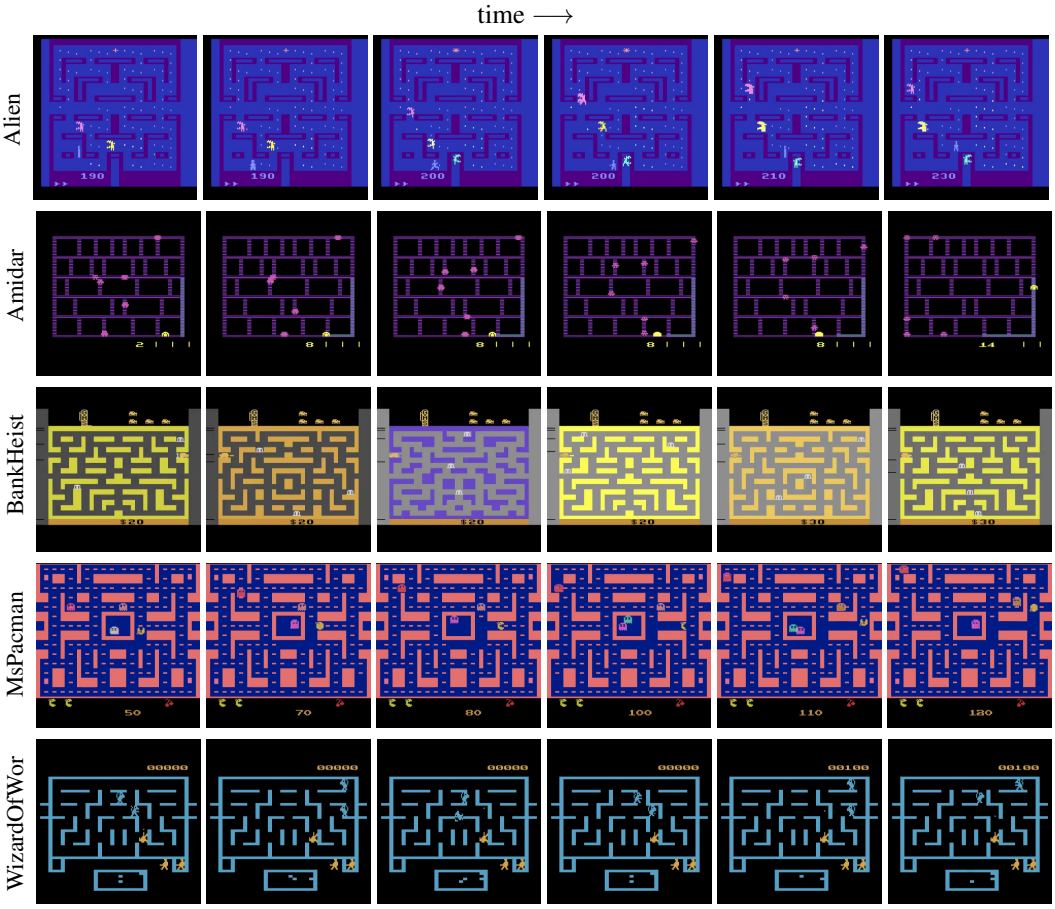

Figure 13. **Visualizations of maze games.**

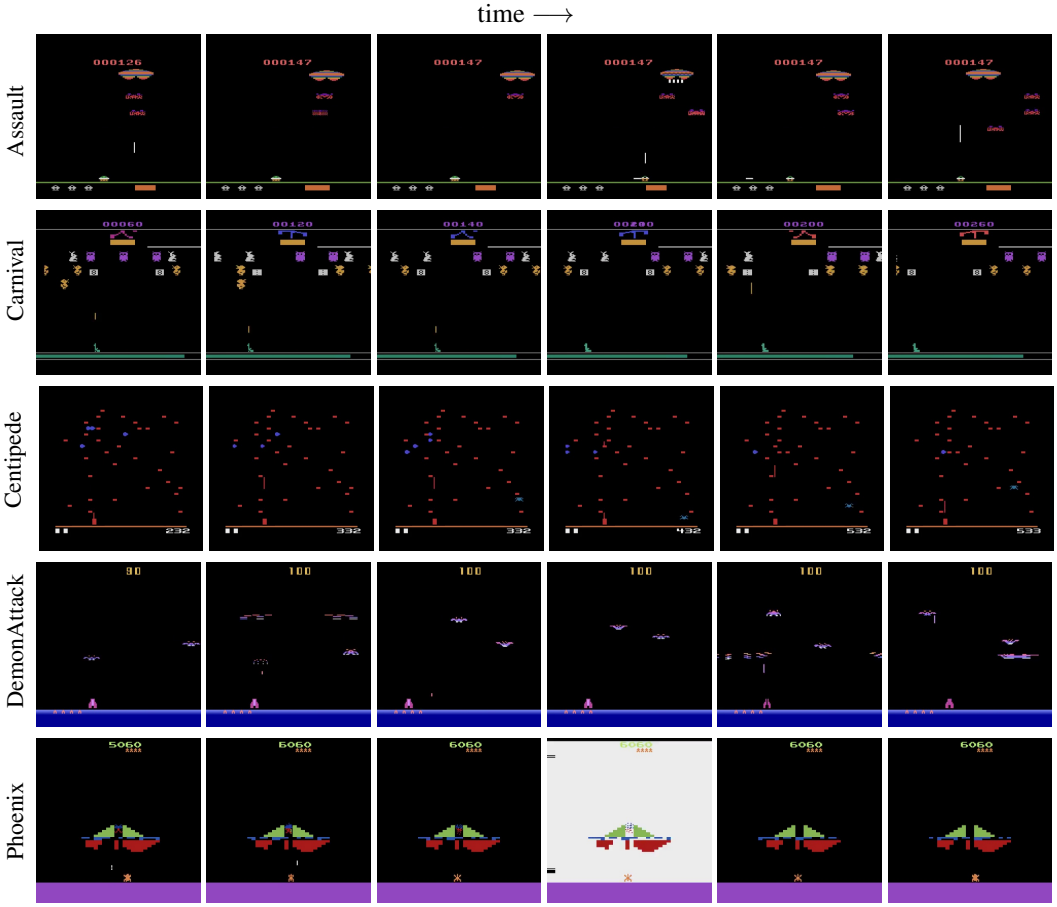

Figure 14. **Visualizations of shooter games.**

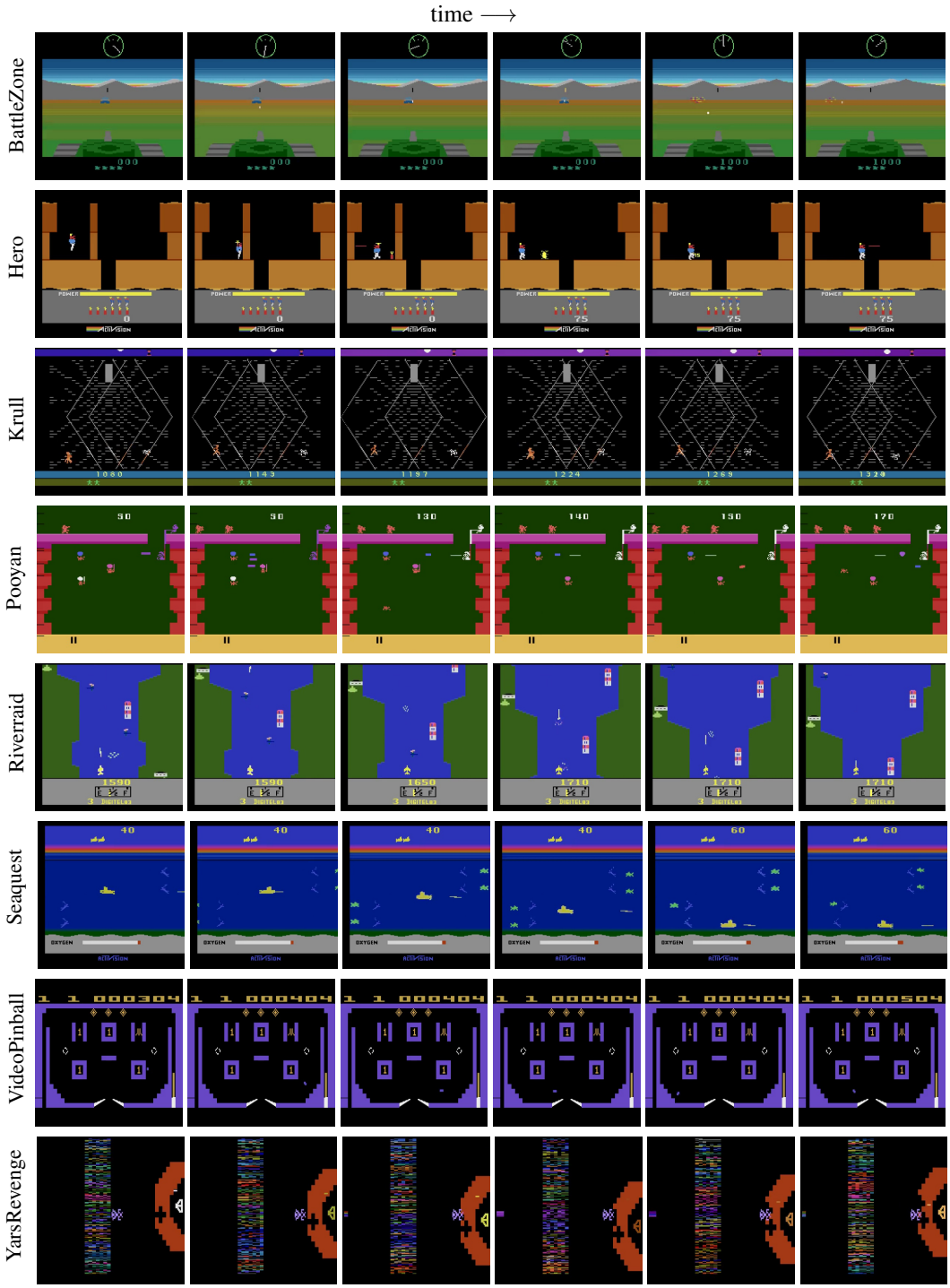

Figure 15. **Visualizations of games from diverse categories.**